Compact high-pulse-energy passively Q-switched Nd:YLF laser with an ultra-low-magnification unstable resonator: application for efficient optical parametric oscillator

C. Y. Cho,[1] Y. P. Huang,[2] Y. J. Huang,[1] Y. C. Chen,[1] K. W. Su,[1] and Y. F. Chen[1,*]

[1]*Department of Electrophysics, National Chiao Tung University, Hsinchu, Taiwan*
[2]*Department of Physics, Soochow University, Shih Lin, Taipei, Taiwan*
[*]*yfchen@cc.nctu.edu.tw*

Abstract: We exploit an ultra-low-magnification unstable resonator to develop a high-pulse-energy side-pumped passively Q-switched Nd:YLF/Cr^{4+}:YAG laser with improving beam quality. A wedged laser crystal is employed in the cavity to control the emissions at 1047 nm and 1053 nm independently through the cavity alignment. The pulse energies at 1047 nm and 1053 nm are found to be 19 mJ and 23 mJ, respectively. The peak powers for both wavelengths are higher than 2 MW. Furthermore, the developed Nd:YLF lasers are employed to pump a monolithic optical parametric oscillator for confirming the applicability in nonlinear wavelength conversions.

OCIS codes: (140.3480) Lasers, diode-pumped; (140.3540) Lasers, Q-switched; (140.3530) Lasers, neodymium.

References and links

1. W. Krichbaumer, H. Herrmann, E. Nagel, R. Häring, J. Streicher, C. Werner, A. Mehnert, T. Halldorsson, S. Heinemann, P. Peuser, and N. P. Schmitt, "A diode-pumped Nd:YAG lidar for airborne cloud measurements," Opt. Laser Technol. **25**(5), 283–287 (1993).
2. D. J. Binks, P. S. Golding, and T. A. King, "Compact all-solid-state high repetition rate tunable ultraviolet source for airborne atmospheric gas sensing," J. Mod. Opt. **47**(11), 1899–1912 (2000).
3. D. Kracht, S. Hahn, R. Huss, J. Neumann, R. Wilhelm, M. Frede, and P. Peuser, "High efficiency, passively Q-switched Nd:YAG MOPA for spaceborne laser-altimetry," Proc. SPIE **6100**, 548–555 (2006).
4. P. Peuser, W. Platz, P. Zeller, T. Brand, M. Haag, and B. Köhler, "High-power, longitudinally fiber-pumped, passively Q-switched Nd:YAG oscillator-amplifier," Opt. Lett. **31**(13), 1991–1993 (2006).
5. C. Bollig, C. Jacobs, M. J. D. Esser, E. H. Bernhardi, and H. M. von Bergmann, "Power and energy scaling of a diode-end-pumped Nd:YLF laser through gain optimization," Opt. Express **18**(13), 13993–14003 (2010).
6. W. A. Clarkson, P. J. Hardman, and D. C. Hanna, "High-power diode-bar end-pumped Nd:YLF laser at 1.053 microm," Opt. Lett. **23**(17), 1363–1365 (1998).
7. Y. J. Huang, Y. S. Tzeng, C. Y. Tang, Y. P. Huang, and Y. F. Chen, "Tunable GHz pulse repetition rate operation in high-power TEM_{00}-mode Nd:YLF lasers at 1047 nm and 1053 nm with self mode locking," Opt. Express **20**(16), 18230–18237 (2012).
8. A. M. Deana, I. M. Ranieri, S. L. Baldochi, and N. U. Wetter, "Compact, diode-side-pumped and Q-switched Nd:$YLiF_4$ laser cavity operating at 1053 nm with diffraction limited beam quality," Appl. Phys. B **106**(4), 877–880 (2012).
9. Y. J. Huang, C. Y. Tang, W. L. Lee, Y. P. Huang, S. C. Huang, and Y. F. Chen, "Efficient passively Q-switched Nd:YLF TEM_{00}-mode laser at 1053 nm: selection of polarization with birefringence," Appl. Phys. B **108**(2), 313–317 (2012).
10. M. S. Ribeiro, D. F. Silva, E. P. Maldonado, W. de Rossi, and D. M. Zezell, "Effects of 1047-nm neodymium laser radiation on skin wound healing," J. Clin. Laser Med. Surg. **20**(1), 37–40 (2002).
11. A. V. Okishev and W. Seka, "Diode-pumped Nd:YLF master oscillator for the 30-kJ (UV), 60-beam OMEGA laser facility," IEEE J. Sel. Top. Quantum Electron. **3**(1), 59–63 (1997).
12. B. Frei and J. E. Balmer, "1053-nm-wavelength selection in a diode-laser-pumped Nd:YLF laser," Appl. Opt. **33**(30), 6942–6946 (1994).
13. H. Zbinden and J. E. Balmer, "Q-switched Nd:YLF laser end pumped by a diode-laser bar," Opt. Lett. **15**(18), 1014–1016 (1990).
14. T. Graf and J. E. Balmer, "High-power Nd:YLF laser end pumped by a diode-laser bar," Opt. Lett. **18**(16), 1317–1319 (1993).

#179633 - $15.00 USD Received 12 Nov 2012; revised 26 Dec 2012; accepted 7 Jan 2013; published 14 Jan 2013

15. C. F. Rae, J. A. C. Terry, B. D. Sinclair, M. H. Dunn, and W. Sibbett, "Single-frequency, end-pumped Nd:YLF laser excited by a 12-mJ diode-laser array," Opt. Lett. **17**(23), 1673–1675 (1992).
16. M. D. Selker, R. S. Afzal, and P. Reichert, "A pulse transmission mode Q-switched Nd:YLF laser pumped by cylindrical microlens-collimated diode bars," IEEE J. Quantum Electron. **30**(7), 1616–1622 (1994).
17. T. Debuisschért, D. Mathieu, J. Raffy, L. Becouarn, E. Lallier, and J.-P. Pocholle, "High beam quality unstable cavity infrared optical parametric oscillator," Proc. SPIE **3267**, 170–180 (1998).
18. R. Beach, J. Davin, S. Mitchell, W. Benett, B. Freitas, R. Solarz, and P. Avizonis, "Passively Q-switched transverse-diode-pumped Nd^{3+}:YLF laser oscillator," Opt. Lett. **17**(2), 124–126 (1992).
19. N. Hodgson and H. Weber, *Laser Resonators and Beam Propagation*, 2nd edn. (Springer, Berlin, 2005), Chap. 5–7.
20. J. E. Murray, "Pulsed Gain and Thermal Lensing of Nd:$LiYF_4$," IEEE J. Quantum Electron. **19**(4), 488–491 (1983).
21. Y. F. Chen, Y. P. Lan, and H. L. Chang, "Analytical Model for Design Criteria of Passively Q-Switched Lasers," IEEE J. Quantum Electron. **37**(3), 462–468 (2001).
22. S. Lee, Y. G. Kim, B. H. Cha, and Y. K. Kim, "A diode-pumped linear intracavity frequency doubled Nd:YAG rod laser with 40 ns pulse width and 73 W green output power," Opt. Laser Technol. **36**(4), 265–271 (2004).
23. Z. Sun, R. Li, Y. Bi, C. Hu, Y. Kong, G. Wang, H. Zhang, and Z. Xu, "Experimental study of high-power pulse side-pumped Nd:YAG laser," Opt. Laser Technol. **37**(2), 163–166 (2005).
24. S. K. Sharma, P. K. Mukhopadhyay, A. Singh, R. Kandasamy, and S. M. Oak, "A simple, compact, and efficient diode-side-pumped linear intracavity frequency doubled Nd:YAG rod laser with 50 ns pulse width and 124 W green output power," Rev. Sci. Instrum. **81**(7), 073104 (2010).

1. Introduction

High-pulse-energy all-solid-state lasers are widely used in scientific research and industrial applications, especially in military respect like airborne laser system, LIDAR and laser target designator, etc [1–4]. Compared to the mostly used Nd:YAG and Nd:YVO_4 crystals, the Nd:YLF crystal having the advantage of longer lifetime is more suitable for high-pulse-energy Q-switched lasers [5,6]. Furthermore, the uniaxial Nd:YLF crystal has two principal lasing transitions at 1047 nm (π) and at 1053 nm (σ), corresponding to the polarizations parallel and perpendicular to the crystal c-axis, respectively [7–9]. The 1047-nm and 1053-nm emissions are of great interest in the skin wound healing [10] and the Nd:glass amplification [11], respectively.

In addition to continuous-wave (CW) pumping, quasi-CW (QCW) diode stacks are often utilized to fulfill Q-switched Nd:YLF lasers with high pulse energies [12–16]. So far, the development of Nd:YLF lasers with energies of several millijoules and approximately 10-ns pulse durations is still highly desirable. Although the end-pumping scheme can permit excellent mode size matching to achieve good beam quality, the limited pump volume usually hinder the scale-up of the output pulse energy. In contrast, the side-pumping scheme can effectively enlarge the pump volume [17, 18]; however, this approach generally suffers from the degradation of beam quality. Therefore, it is practically valuable to develop a side-pumped Nd:YLF laser with improving beam quality.

The thermal lensing effect of the Nd:YLF crystal is identified to be relatively weak due to the compensation of negative temperature dependence of the refractive index and positive temperature dependence of the thermal expansion coefficient. In this work, we employ the property of the weak thermal lens with an ultra-low-magnification unstable resonator to develop a compact high-pulse-energy side-pumped passively Q-switched Nd:YLF/Cr^{4+}:YAG laser with improving beam quality. We also use the birefringent characteristics of an one-end-wedge a-cut Nd:YLF crystal to independently obtain the laser transitions at 1047 nm and 1053 nm through the cavity alignment. Using a Cr^{4+}:YAG crystal with initial transmission of 70% and at a repetition rate of 10 Hz, the pulse energies at 1053 nm and 1047 nm reach 23 mJ and 19 mJ, respectively. With the experimental pulse durations, the peak powers are calculated to be up to 2.3 MW and 2.7 MW at the emissions of 1053 nm and 1047 nm, respectively. The beam-quality factors M^2 are measured to be approximately 3.5 × 5.5 and 3.5 × 6.8 (vertical × horizontal) for the emissions at 1053 nm and 1047 nm, respectively. Furthermore, the developed Nd:YLF laser is employed to pump a monolithic optical parametric oscillator (OPO). The pulse energies generated in the external OPO are 10 mJ and 5.5 mJ for the wavelengths at 1552 nm and 1541 nm, respectively.

#179633 - $15.00 USD Received 12 Nov 2012; revised 26 Dec 2012; accepted 7 Jan 2013; published 14 Jan 2013

2. Cavity design and setup

For the cavity design, we first consider an optical resonator that consists of one laser crystal with thermally focal length f_{th} and two mirrors with radii of curvature ρ_1 and ρ_2 separated by an optical distance L. In term of the g^*-parameters, the beam radii ω_1 and ω_2 on the two mirrors can be expressed as [19]:

$$\omega_i = \sqrt{\frac{\lambda L^*}{\pi}} \sqrt{\frac{g_j^*}{g_i^*(1-g_1^* g_2^*)}}; i, j = 1,2; i \neq j, \tag{1}$$

where

$$g_i^* = g_i - \frac{d_j}{f_{th}}\left(1-\frac{d_i}{\rho_i}\right), \tag{2}$$

$$g_i = 1-\frac{d_1+d_2}{\rho_i}; i, j = 1,2; i \neq j, \tag{3}$$

$$L^* = d_1 + d_2 - \frac{d_1 d_2}{f_{th}}. \tag{4}$$

Here d_1 and d_2 are the optical path length between the cavity mirrors and the principal planes of the laser crystal. For the subsequent analysis, we specifically focus on the case of $d_1 = d_2 = L/2$. For the QCW pumping and the weak thermal lensing effect of the Nd:YLF crystal, the cavity length can be realistically designed to satisfy the condition of $L << f_{th}$. In order to obtain a large mode volume, we use an ultra-low-magnification positive-branch unstable cavity to design the resonator under the circumstance of $f_{th} \to \infty$. For the convenience of further discussion, we use the expression of $g_1 g_2 = 1 + \varepsilon$ with $0 < \varepsilon << 1$ to represent the cavity form.

With the conditions of $d_1 = d_2 = L/2$, $L << f_{th}$ and $g_1 g_2 = 1 + \varepsilon$, we can obtain that $g_1^* g_2^* \approx 1 - \Delta$, where

$$\Delta = \left(\frac{L}{f_{th}}\right)\left(\frac{g_1 + g_2 + 2g_1 g_2}{4}\right) - \varepsilon. \tag{5}$$

Equation (5) indicates that when the thermally focal length f_{th} of the gain medium makes the cavity to reach the condition of $\Delta \geq 0$ in the pumping stage, the laser resonator starts to be driven into the stable regime. As long as the factor Δ can satisfy the criterion of $0 < \Delta << 1$ in the lasing stage, the cavity mode sizes can be maintained fairly large, as indicated in Eq. (1).

We employ a convex-concave cavity to realize the criterion mentioned above. A convex mirror with the radius of curvature of 500 mm was used as the rear mirror of the cavity that was coated for high reflection (R>99.8%) in the range of 1040-1060 nm. A concave mirror with the radius curvature of 600 mm was used as the output coupler of the cavity that was coated for partial reflection in the range of 1040-1060 nm. We chose the effective cavity length L to be 90 mm. Consequently, the factor of $g_1 g_2$ can be calculated to be 1.003, i.e. $\varepsilon = 0.003$. In terms of the parameter ε, the magnification of the unstable resonator is given by $M \approx 1 + (2\varepsilon)^{0.5} + \varepsilon$. As a result, the magnification can be calculated to be approximately 1.08, corresponding to an ultra-low-magnification unstable resonator. It is worth to mention that for typical unstable resonators, larger magnification leads to a smaller misalignment sensitivity. Although the present cavity design is an unstable resonator with an ultra-low magnification, however, with appropriate thermal lensing effect in the laser crystal, it can step into the stable regime and possess a large mode volume. Therefore, the misalignment sensitivity is not rather critical. With Eq. (5), we can find that to step into the stable regime, the thermally focal

#179633 - $15.00 USD Received 12 Nov 2012; revised 26 Dec 2012; accepted 7 Jan 2013; published 14 Jan 2013

length f_{th} is approximately smaller than 30 m. This feature is quite appropriated for Nd:YLF crystal which has relatively weak thermal lensing effect [12, 20].

The experimental set-up for the Nd:YLF laser is schematically shown in Fig. 1. The laser crystal was a 1.0 at. % a-cut Nd:YLF crystal with dimension of 4 × 3 × 12 mm^3. The second end facet was cut with 3°-wedged to prevent the parasitic effect and to separate two wavelengths. Both end facets of the laser crystal were coated for anti-reflection (R<0.2%) at 1050 nm and its pump face was coated for anti-reflection (R<0.2%) at 808 nm. A Cr^{4+}:YAG crystal was applied for passively Q-switching as the saturable absorber. Both facets of the saturable absorber was coated for anti-reflection (R<0.2%) coating at 1050 nm. All crystals were wrapped with indium foil and mounted in conductively cooled copper blocks. The pump source was a high-power diode stacks (Coherent G-stack package, Santa Clara, Calif., USA), consisted of six 10-mm-long diode bars. Pitch between each diode bar was 0.4 mm, so the whole emission area was approximately 10 × 2.4 mm^2. The full divergence angles in the fast and slow axes were approximately 35° and 10°, respectively. The diode stack was placed close to the lateral surface of the laser crystal to receive good pump efficiency. In this work, pumping pulse width and pumping repetition rate of the diode stacks were all set to be 500 μs and 10 Hz. The pulse temporal behaviors were recorded by a LeCroy digital oscilloscope (Wavepro 7100, 10 G samples/s, 1 GHz bandwidth) with a fast InGaAs photodiode. The emission wavelengths were recorded by an ADVANTEST optical spectrum analyzer with resolution of 0.1 nm (Q89381A).

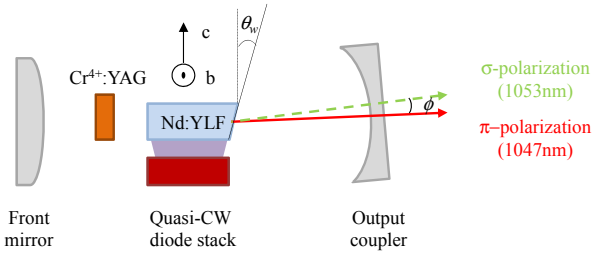

Fig. 1. Experimental set-up of Nd:YLF laser.

Before carrying on the experiment, we estimated the output performance of the passively Q-switched laser at two wavelengths to determine the parameters of the output coupler and the saturable absorber. We simply applied the analytical models in Ref. 21 for simulations. The reflectivity of the output coupler was chosen to be larger than 70% considering the higher pumping threshold at 1053 nm and the limitation of pumping source. In order to maintain the similar pulse energies at two wavelengths, the initial transmission of saturable absorber was chosen to be approximately 70%. Assuming the pumping mode radius was approximately 1.5 mm, the calculated output pulse energies at 1047 nm and 1053 nm were 17 mJ and 26 mJ.

3. Experimental results for laser performance

At first, we performed the QCW free-running without the Cr^{4+}:YAG crystal to confirm the reliability of the laser configuration and the quality of the laser crystal. We verified that tilting the orientation of the output coupler was able to switch the output wavelength of Nd:YLF laser. Figure 2 shows the curve of the laser output energies at 1047 nm and 1053 nm versus input energy of laser diode stacks under QCW free-running operation. The pump thresholds of 1047 nm and 1053 nm were 60 mJ and 96 mJ. With the pumping energy of 357 mJ, the output energies were 56 mJ and 48 mJ at 1047 nm and 1053 nm, respectively. The slope efficiency at 1047 nm and 1053 nm were both approximately 22%.

#179633 - $15.00 USD Received 12 Nov 2012; revised 26 Dec 2012; accepted 7 Jan 2013; published 14 Jan 2013

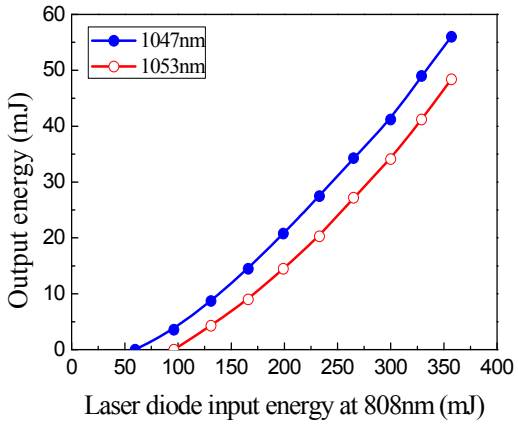

Fig. 2. Output energies under free-running operation with respected to the launched pump energies.

Then we inserted Cr^{4+}:YAG crystal to observe the performance of passively Q-switching at 1047 nm and 1053 nm, respectively. Since the threshold of Nd:YLF crystal at 1047 nm was lower than that at 1053 nm, we studied the performance at 1047 nm first. The pump threshold energy was measured to be 272 mJ with the output pulse energy about 19 mJ. The temporal shape of the passively Q-switched pulse at 1047 nm is depicted in Fig. 3 (a), which displays the frequency-beating modulation. The pulse width was approximately 9 ns. With the recorded data of pulse shape, the peak power was numerically calculated to be approximately 2.7 MW. We adjusted the output coupler to align the cavity for laser emission at 1053 nm. The output pulse energy was found to be 23 mJ in the passively Q-switched operation with the pump threshold energy of 357 mJ. Although the pump threshold energy at 1053 nm was higher than that at 1047 nm, which comes from the lower emission cross section, the output energy at 1053 nm was approximately 1.2 times higher than that at 1047 nm. The temporal shape of the passively Q-switched pulse at 1053 nm is depicted in Fig. 3(b). The pulse width was approximately 10 ns, and the peak power was numerically calculated to be approximately 2.3 MW.

Compared to the simulations, the experimental pulse energy at 1047 nm was larger, which was opposite at 1053 nm. We suspected that it was due to the different mode volumes in two wavelengths. According to previous works [12, 20], the thermal lensing effect in Nd:YLF crystal was relatively weak at 1047 nm than at 1053 nm, which contributed to a smaller thermally focusing length f_{th}. Furthermore, the higher threshold energy at 1053-nm transition increased the thermal lensing effect. Combining with Eq. (1), which implied that smaller f_{th} corresponds to a smaller mode radius, the cavity mode size at 1047-nm transition would be larger than that at 1053 nm. As a consequence, the experimental results should be modified considering the different mode areas.

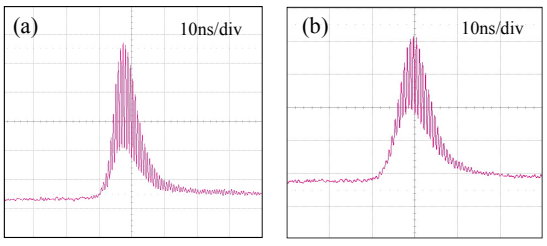

Fig. 3. Temporal shape for the laser pulses in the single pulse regime at (a) 1047 nm and (b) 1053 nm.

#179633 - $15.00 USD Received 12 Nov 2012; revised 26 Dec 2012; accepted 7 Jan 2013; published 14 Jan 2013

Figures 4(a) and 4(b) show the transverse mode distributions for the passively Q-switched lasers at 1047 nm and 1053 nm, respectively. It can be seen that the transverse pattern at 1053 nm is quite close to a Gaussian mode, whereas the mode structure at 1047 nm displays somewhat high-order modes. We employed the z-scan method to evaluate the beam quality. The beam quality factors M^2 at 1047 nm and 1053 nm were measured to be 3.5 × 6.8 and 3.5 × 5.5 (vertical × horizontal), respectively. As observed in the transverse patterns, the beam quality at 1053 nm is considerably better than that at 1047 nm in the horizontal direction. This result may arise from the fact that the temperature dependence of the refractive index for the 1053-nm emission is smaller than that for the 1047-nm emission. To compare the beam qualities, we simply replaced the convex rear mirror for a plane mirror, which allow the resonator to be in stable region. Through the experiment, we found that the beam quality factors $M_x \times M_y$ were measured to be larger than 30 × 10 at both wavelengths. Worse of all, the transverse patterns appeared to be both high-order modes. It is also worthwhile to mention that the beam quality factors obtained with the unstable cavity design are significantly improved as compared with the previous side-pumped solid-state lasers of the similar linear-cavity configuration [22–24]. In the following, we utilized the present Nd:YLF Q-switched lasers to pump an OPO cavity formed by a monolithic KTP crystal to confirm the application in nonlinear wavelength conversions.

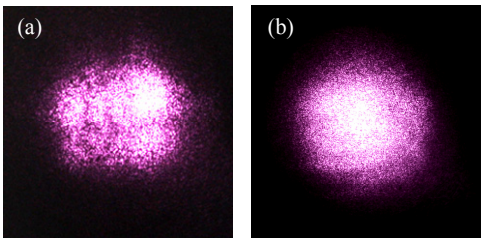

Fig. 4. Output transverse mode distributions at (a) 1047 nm and (b) 1053 nm.

The nonlinear crystal for the external OPO was an x-cut KTP with dimension of 4 × 4 × 20 mm^3. The first end facet was coated for high-transmission (T>95%) in the range of 1040-1060 nm and high-reflection (R>99.8%) in the range of 1540-1560 nm. The second end facet was coated for anti-reflection (R<0.2%) in the range of 1040-1060 nm and partial-reflection (R = 80%) within 1540-1560 nm. The KTP crystal was wrapped with indium foil and mounted in a conductively cooled copper block. An EOT isolator (1030 nm ~1080 nm) was used to prevent the depleted pump light getting back to the resonance. The effective transmission of the isolator was found to be approximately 92%.

After passing through the isolator, the pulse energies at 1053 nm and 1047 nm were 21.5 mJ and 17.5 mJ, operating at the same condition as the passively Q-switched laser. The output wavelength of external OPO pumped by the 1053 nm laser was found to be 1552 nm and the pulse energy was up to 10 mJ, corresponding to an optical-to-optical efficiency of 44%. With the temporal distribution, the peak power was numerically calculated to be 0.88 MW. On the other hand, the output wavelength of external OPO pumped by the 1047 nm laser was 1541 nm and the pulse energy was found to be 5.5 mJ, corresponding to an optical-to-optical efficiency of 28%. The peak power at 1541 nm was measured to be 0.63 MW. The higher conversion efficiency with 1053 nm laser is mainly due to the better beam quality. The oscilloscope traces are depicted in Fig. 5. It can be found that the mode-locking modulations in the temporal shapes of the fundamental light sources are effectively cleaned through the OPO process

#179633 - $15.00 USD Received 12 Nov 2012; revised 26 Dec 2012; accepted 7 Jan 2013; published 14 Jan 2013

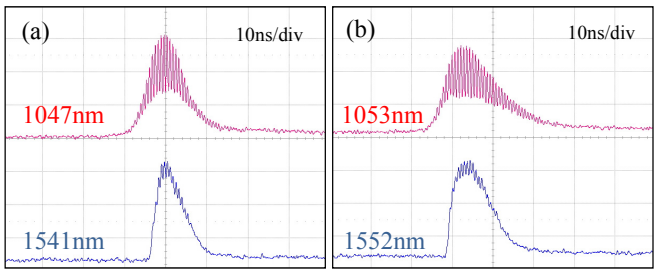

Fig. 5. Temporal shape for the pump pulses and signal pulses of external OPO at (a) 1047 nm and (b) 1053 nm.

4. Conclusion

An ultra-low-magnification unstable cavity has been used to develop a high-pulse-energy side-pumped Nd:YLF passively Q-switched laser with improving beam quality. With the birefringent property of a wedged gain medium, the laser cavity can be independently adjusted to obtain the emissions at 1047 nm and 1053 nm. With a Cr^{4+}:YAG crystal of initial transmission of 70%, the pulse energies at a repetition rate of 10 Hz are found to be 23 mJ and 19 mJ for the emissions at 1053 nm and 1047 nm, respectively. With the temporal pulse shapes, the peak powers for the emissions at 1053 nm and 1047 nm were evaluated to be up to 2.3 MW and 2.7 MW, respectively. With the z-scan method, the beam-quality factors M^2 are found to be 3.5 × 5.5 and 3.5 × 6.8 (vertical × horizontal) for the emissions at1053 nm and 1047 nm, respectively. Moreover, the developed Nd:YLF laser is used to pump a monolithic optical parametric oscillator (OPO) to generate the pulse energies of 10 mJ and 5.5 mJ for the wavelengths at 1552 nm and 1541 nm, respectively.

Acknowledgments

The authors thank the National Science Council for the financial support of this research under Contract No. NSC100-2628-M-009-001-MY3.

#179633 - $15.00 USD Received 12 Nov 2012; revised 26 Dec 2012; accepted 7 Jan 2013; published 14 Jan 2013